

Structural Transitions in Polyriboadenylic Acid Induced by the Changes in pH and Temperature: Vibrational Circular Dichroism Study in Solution and Film States

Ana G. Petrovic and Prasad L. Polavarapu*

Department of Chemistry, Vanderbilt University, Nashville, Tennessee 37235

Received: August 2, 2005; In Final Form: October 18, 2005

A correlation of the changes in vibrational absorption and vibrational circular dichroism (VCD) spectral features with the structural changes of polyriboadenylic acid (polyA) as a function of pH is reported. Analysis of the solution spectral data as a function of pH led us to establishing the importance of a previously unrecognized absorption band at $\sim 1665\text{ cm}^{-1}$. The present studies indicate that this absorption band and associated VCD originate from the double-helical structure of polyA. The observed changes in solution-state VCD features are indicative of the pH-dependent transitions among the three acidic forms of polyA (A, B, and “frozen” form). In addition to the solution-state spectral data, pH-dependent absorption and VCD spectra for films of polyA, derived from dilute H_2O solutions, are also presented. The pH-dependent changes in the absorption and VCD spectra of films are also correlated to the polyA structural changes.

Introduction

Nucleic acids and their constituents play key roles in the storage and transmission of genetic information in all cells, in the readout of this information during protein synthesis, and in many metabolic processes.¹ Because of their importance in biological processes, nucleic acids have been subjected to a number of investigations. Considerable amount of effort has been made toward establishing the relationship between their structure and function. Over the years, the structural elucidation of nucleic acids, including polyadenylic acid (polyA), has been the goal of a number of spectroscopic techniques, with varying degrees of success. PolyA (Figure 1), a homopolynucleotide, is a constituent of mRNA of all living organisms, and it has been established that polyA participates in several processes² including mRNA transportation from nucleus to cytoplasm, degradation, and translation initiation. The study of structural and conformational transitions of polyA is deemed important for a better understanding of the structure–function relationship in naturally occurring nucleic acids.

Early work on the structural elucidation of polyA included X-ray diffraction studies,^{3,4} ultraviolet (UV) spectroscopy,^{5–8} optical rotatory dispersion (ORD)^{9a,10–13}, electronic circular dichroism (ECD)^{8,14–16}, and nuclear magnetic resonance (NMR).^{17–19} On the basis of the previous studies it has been concluded that polyA exhibits two secondary structures depending on the pH. On the basis of sedimentation constants and viscosities, Fresco and Doty²⁰ noted that polyA undergoes structural changes when going from neutral to acidic conditions. The structure of polyA at alkaline and neutral pH was suggested to be a right-handed single-stranded helix, stabilized by the stacked array of bases with their planes nearly perpendicular to the helix axis.^{9a,14,16} There is no evidence²¹ for internucleotide hydrogen bonding in the neutral, single-helical form. In support of this structure, NMR data²² of the adenine protons showed chemical shifts that are analogous to those found in other systems of stacked aromatic rings. UV-ECD²³ and ORD data^{9a}

displayed the behavior expected for stacked chromophores with transition moments perpendicular to the helix axis. At acidic pH, however, polyA exhibits a right-handed double-stranded helical structure with parallel chains and stacked protonated bases.^{3,6,20} The bases are tilted^{3,9a} with respect to the helical axis. Each nucleotide is held in place by stacking interaction with adjacent bases as well as by hydrogen bonds to the other chain. The double-stranded form contains eight nucleotide pairs per helix turn.^{1,15} Several observations have been cited in support of the double helix. On the basis of the X-ray diffraction studies, Rich et al.³ have proposed that the double-stranded structure is stabilized by the electrostatic attraction between the positively charged protons at the $\text{N}_{(1)}$ atoms of the adenines and the negatively charged phosphate groups (Figure 2). On the basis of correlations between hydrogen-ion titration data and thermal denaturation curves, Holcomb and Timasheff^{8b} later reconfirmed the idea of the double-helix stabilization through electrostatic interactions. As depicted in Figure 2, two parallel strands are held together by four hydrogen bonds per base pair, two of which are between $\text{N}_{(10)}\text{H}_2$ and $\text{N}_{(7)}$ and the other two are between $\text{N}_{(10)}\text{H}_2$ and a phosphate oxygen.³ Furthermore, small-angle X-ray scattering measurements⁴ showed that the mass per unit length of the neutral structure is one-half of that in the acidic structure, which represents a convincing evidence concerning single- versus double-helix structural differences associated with changes in pH.

A structural transition from the neutral, single-strand structure to the acidic, double-strand structure was reported to occur at a pH near the pK_a of 5.87 for polyA, as inferred from UV absorption, ORD, and ECD.²⁴ Interestingly, as originally determined from the X-ray data by Rich et al.,³ full protonation is not a structural requirement for the acidic structure of polyA. Namely, depending on the extent of protonation of the molecule, three different acidic conformations are found for polyA: B form, A form, and “frozen” form.^{25–27} The least acidic of the three forms (at higher pH) is designated as the B form, also known as an “intermediate”²⁵ form, which is considered to be stable near half-protonation. Form B is the only structure present at a pH just below pK_a , associated with the partial protonation

* Author to whom correspondence should be addressed. Phone: (615)-322-2836. Fax: (615)322-4936. E-mail: Prasad.L.Polavarapu@vanderbilt.edu.

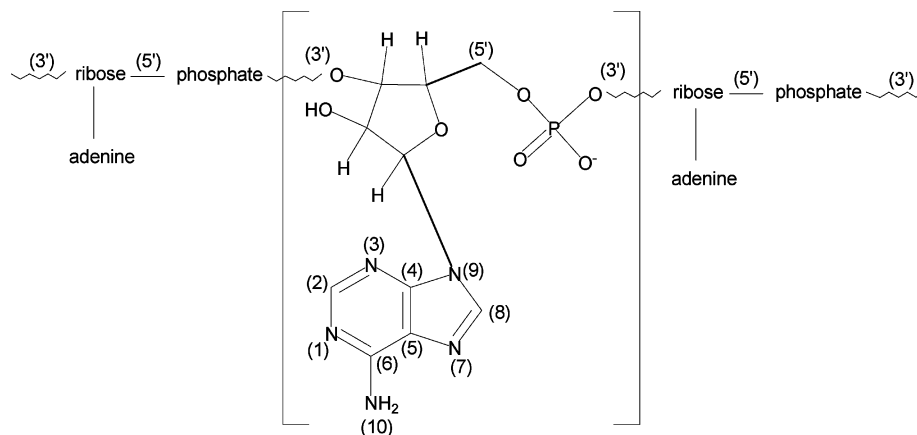


Figure 1. Chemical structure of a monomer unit of the polyadenylic acid (polyA). The atom numbers shown are used in the text to define hydrogen bonding and electrostatic interactions.

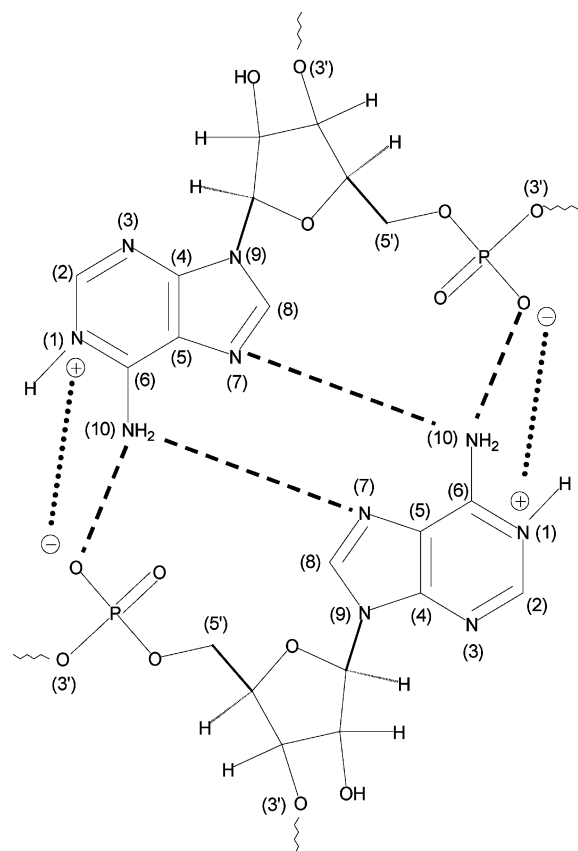


Figure 2. Interaction of two monomer units belonging to complementary chains of polyA, when found in an acidic environment. Hydrogen bonds are designated with broken lines, while electrostatic interactions are given by dotted lines.

of adenine moieties. At pH 5.81, ORD²⁴ of polyA indicates the B form. As the pH is further lowered, there is a gradual conversion of form B into form A. Form A, also known as the “tightly packed” form, is stable at complete protonation of adenine constituents. At pH 4.00, ORD²⁴ of polyA indicates the pure A form. Finally, the third and the most acidic form, known as the “frozen” form, is created from neutral polyA at low pH (<3.8).²⁵ According to previous studies,^{25–27} the frozen form represents a gridlike aggregate consisting of alternating, variably sized, single-stranded regions linked with short double-stranded regions. The prevention²⁷ of formation of the frozen form can be accomplished by a slow dialysis of single-strand solution against an acidic solvent. Additionally, the frozen form of aggregated polyA can be destroyed^{25,26} by heating, which

promotes the process of separation of strands and their recombination in a more ordered manner. Despite the fact that a wide variety of physical and chemical techniques have been employed in the past to elucidate the structural assignment for polyA as a function of pH, we could not find any report on how infrared (IR) vibrational absorption and vibrational circular dichroism (VCD) spectral features reflect structural changes of polyA as a function of pH. The only IR and VCD spectra of polyA that have been reported^{28–32} in the past are of solution-state polyA at or near neutral pH.

VCD spectroscopy has the potential for revealing the conformations of nucleic acids.^{28,30–34} VCD features associated with numerous spectrally resolved vibrational bands provide a large database for structural interpretations. The vibrational bands in the $\sim 1750\text{--}1600\text{ cm}^{-1}$ region originate from in-plane base vibrational modes of nucleic acids. The interactions between these vibrations are strongly dependent on geometrical factors and thus give rise to VCD signals that reveal the nature of base stacking interactions. VCD is also sensitive to the helical handedness of nucleic acids.^{33b}

In this paper we report the pH-dependent IR and VCD spectra of polyA, in both solution and film states, for the first time and deduce the structural/conformational changes from these spectra.

Experimental Section

The polyA potassium salt (P9403), and D-(+)-trehalose were obtained from Sigma Chemical Co. and have been used as received. D₂O was obtained from Cambridge Isotope Laboratories, Inc.

Liquid solution samples, at a final concentration of $\sim 18\text{ mg/mL}$, were prepared by dissolving polyA in 0.1 M NaCl solution, containing 10 mM citrate buffer (for pH $\sim 3.5\text{--}6.0$) or Tris buffer (for pH ~ 8.0) in D₂O. A glass-body liquid-filled microcombination pH electrode was used for all pH readings. No corrections were made for the differences between pH and pD. The 10 mM concentration of citric acid is low enough for the absorption associated with its carbonyl group not to interfere with the base vibrational bands. PolyA is prone to gel formation at higher concentrations, in acidic environment. For the concentration used here, polyA solution became increasingly more viscous as the pH was lowered. At pH 4.0, it was considerably viscous but could be drawn out with a pipet. At pH 3.5, the polyA solution had a gellike appearance and was transparent.

For each of the pH values considered, IR and VCD spectra of polyA solution have been measured at room temperature ($\sim 22\text{ }^{\circ}\text{C}$), at an elevated temperature ($\sim 70\text{ }^{\circ}\text{C}$), and back at

room temperature (after allowing for 1 h of cooling time). This thermal cycling was used to establish whether the conformational change during heating is reversible upon cooling. Heating was accomplished by holding the sample in a variable temperature cell. The temperatures were read with a thermocouple embedded in the cell. The aggregated sample solution at pH 3.5 was additionally heated to $\sim 110^\circ\text{C}$ for approximately 5 min, and the spectra were taken after allowing the sample to equilibrate back to room temperature.

For preparation of the film samples a drop-cast method was used, where $\sim 200\ \mu\text{L}$ of parent aqueous solution, at a concentration of $\sim 6\ \text{mg/mL}$, was deposited on a 2.5 cm diameter CaF_2 window and allowed to dry at room temperature for approximately 2–3 h in a fume hood, which provided a constant airflow over the sample. Trehalose was added to the polyA solution at a mass ratio of 2:1 (trehalose/polyA). The pH of the parent solutions was adjusted in the same manner as for the solution study. The difference in preparation of the solution and film state samples was that for film samples the solution buffer concentration was $\sim 5\ \text{mM}$ and no NaCl was included to avoid its precipitation on the surface of the film. Films were tested for orientational dependence by taking the spectra at two positions: an arbitrarily chosen 0° position and a position corresponding to 45° rotation around the light beam axis.

IR and VCD measurements for both solution and film state samples were obtained on a modified ChiralIR (Bomem-Biotech, Canada) instrument using the double polarization modulation method, a ZnSe beam splitter, a BaF_2 polarizer, an optical filter (transmitting below $2000\ \text{cm}^{-1}$) and a $2 \times 2\ \text{mm}^2$ HgCdTe detector. All VCD spectra were recorded for 1 h of data collection time, at $8\ \text{cm}^{-1}$ resolution. The solution sample was held in a demountable cell with CaF_2 windows and a $50\ \mu\text{m}$ Teflon spacer. Baseline corrections for all solution-based absorption (or VCD) spectra were done by subtracting the absorption (or VCD) of the buffered D_2O solvent, containing NaCl.

A Zeiss Axiovert 200 M Inverted Fluorescence Microscope was used for obtaining microscopic pictures of the film state samples of polyA.

Results and Discussion

Solution-State Measurements. The pH-dependent IR absorption (A) and VCD (B) spectra in the 1800 and $1300\ \text{cm}^{-1}$ region measured at room temperature (22°C) and at a higher temperature (70°C) are shown in Figure 3. The region below $1300\ \text{cm}^{-1}$ is not displayed due to strong interference from D_2O . Figure 3 indicates that lowering of the pH from 8.0 to 3.5 leads to continuous changes in the spectral features.

There are four absorption bands, labeled as I–IV in Figure 3A, that exhibit notable changes as a function of pH. The most pronounced changes are seen for band I at $\sim 1665\ \text{cm}^{-1}$, which undergoes a considerable increase in intensity as the pH is lowered. Band I is of particular interest here because this band was not recognized^{32,34} in the literature theoretical analyses, perhaps due to its absence in some measurements under apparently similar experimental conditions. Specifically, absorption band I was present in the spectra reported in refs 28a and 32 but was absent in the spectra reported in refs 28b and 29–31. The reasons for the appearance/disappearance of band I and its vibrational origin were not discussed, and this band was excluded^{32,34} from the spectral analysis.

As the acidity of the solution increases, the following structural changes were reported³ to take place: atom $\text{N}_{(1)}$ of the adenine ring becomes protonated (with D in place of H in

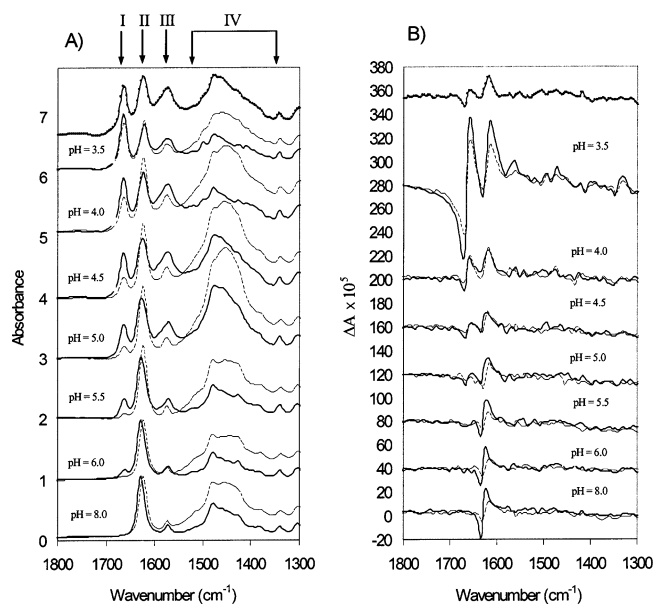


Figure 3. Solution-based vibrational absorption (A) and circular dichroism (B) spectra of polyA in the pH range of 8.0–3.5. The traces given by the straight line correspond to spectra taken at room temperature (22°C), while the traces given by the broken line correspond to spectra taken at elevated temperature (70°C). The topmost trace corresponds to a spectrum taken when the sample at pH 3.5 was heated to 110°C and then cooled back to room temperature. See text for further details.

D_2O), thus resulting in the development of a positive charge that can form favorable electrostatic interactions with the phosphate moiety; atom $\text{N}_{(7)}$ of one polyA chain begins hydrogen bonding with $\text{N}_{(10)}\text{H}_2$ of another polyA chain (Figure 2), which gives rise to intertwining of the two chains and stabilization of the double-helical structure; $\text{N}_{(10)}\text{H}_2$ additionally stabilizes the double-helical structure by participating in the hydrogen bonding with oxygen belonging to the phosphate moiety of the complementary polyA chain. These changes become reinforced as the environment becomes increasingly more acidic.

On the basis of the tabulated correlations^{35,36} between various types of vibrational modes and typical frequency ranges where these modes occur, the origin of band I can be associated with $\text{C}=\text{N}$ ($\text{C}_{(2)}=\text{N}_{(3)}$, $\text{C}_{(6)}=\text{N}_{(1)}$, $\text{C}_{(8)}=\text{N}_{(7)}$; see Figure 1) stretching vibrations with contributions from $\text{N}_{(10)}\text{H}_2$ bending vibrations. Since the origin of band I is associated with vibrations of atoms undergoing the above-mentioned modifications, it is not surprising that this band undergoes a considerable change in its intensity as the pH is lowered. The magnitude of band I becomes intensified with the formation of a double helix in the acidic environment. The intensity of band I represents a direct measure of the degree of adenine ring protonation and, hence, double-helix formation. The observation that the IR spectrum at pH 8.0 does not exhibit band I and that at pH 6.0 this band starts to grow can be taken as the diagnostic marker for the double-stranded helical structures of polyA. This identification was not reported to date.

It should be noted that among the previously reported studies, aside from band I, the remaining bands for polyA were reproduced. For instance, good reproducibility is displayed for band II, which is located at $\sim 1628\ \text{cm}^{-1}$ and previously received much attention because it gives the rise to a strong, sharp, positive VCD couplet at neutral pH. Some literature studies of polyA in a neutral aqueous environment have assigned^{28–30} the origin of band II to $\text{C}_{(4)}=\text{C}_{(5)}/\text{C}_{(5)}-\text{C}_{(6)}$ stretching motions.

Nevertheless, in a recent study³² Andrushchenko et al. correlated the *ab initio* calculated normal vibrational modes of an octamer (rA)₈ with experimental IR bands of polyA in D₂O and indicated that the band at $\sim 1628\text{ cm}^{-1}$ originates from adenine ring C=N stretches coupled to N—D vibrational deformations. Furthermore, the *ab initio* predicted³² theoretical absorption and VCD spectra of (rA)₈, with properties transferred from adenine surrounded by five D₂O molecules, are in good agreement with the D₂O-based experimental spectral features of poly A reported here at basic pH.

In terms of the pH-dependent changes, band II undergoes a twofold change. First, its intensity gradually decreases as the pH is lowered, but this decrease is not as pronounced as the increase in intensity of band I. Second, while band II remains centered at $\sim 1628\text{ cm}^{-1}$ over the pH range of 5.5–8.0, its position gradually shifts to $\sim 1627\text{ cm}^{-1}$ at pH 5.0, to $\sim 1624\text{ cm}^{-1}$ at pH 4.5 and 4.0, and finally, to $\sim 1621\text{ cm}^{-1}$ at pH 3.5. The gradual transformation of band II in both magnitude and position reflects the transformation from the less protonated, acidic form B to the more protonated, acidic form A. It should be noted that the ability to differentiate between forms A, B, and the frozen form is easier based on the VCD spectral features (*vide infra*).

Band III, located at $\sim 1573\text{ cm}^{-1}$, undergoes the least notable change. Its intensity and position remain essentially the same during pH transitions, yet the peak shape somewhat broadens as the pH decreases. On the basis of the correlation between IR spectra of the octameric (rA)₈ model and polyA, Andrushchenko et al.³² suggested that band III is predominantly due to C=N stretching vibration.

Unlike the three bands noted in the region between 1700 and 1550 cm^{-1} , whose changes are gradual and with a clear transition in tendencies as the pH is lowered, the frequency region labeled as IV, between 1550 and 1350 cm^{-1} , is not very useful for structural interpretation because the broad unresolvable features here may arise from D₂O or HDO. The two spectra at pH 6.0 and 5.5 resemble each other, as do those at pH 5.0 and 4.5, and those at pH 4.0 and 3.5. The spectral features at pH 8.0 seem to best resemble those at pH 6.0 and 5.5.

More transparent evidence for the existence of three distinguishable conformations can be seen in the pH-dependent VCD spectra displayed in Figure 3B. At pH 8.0 and 6.0, absorption band II, observed at $\sim 1628\text{ cm}^{-1}$, gives rise to a sharp, positive VCD couplet of equal intensities for negative and positive lobes. As the pH is lowered to 5.5, the positive couplet centered at $\sim 1628\text{ cm}^{-1}$ remains but with a slight decrease in intensity and a shift of the positive lobe from ~ 1624 to $\sim 1622\text{ cm}^{-1}$. In addition, band I at $\sim 1665\text{ cm}^{-1}$ begins to develop a negative VCD contribution at pH 5.5. As the pH is further lowered to 5.0, not only does this negative VCD band become well-defined, but also a positive VCD contribution is developed at a slightly lower frequency. These two VCD contributions appear to form another conservative, positive VCD couplet at $\sim 1665\text{ cm}^{-1}$. At pH 4.5 and especially 4.0, the newly developed positive couplet becomes dominant, while the positive couplet at $\sim 1628\text{ cm}^{-1}$ is diminished in intensity, giving the appearance of a positive band centered at $\sim 1618\text{ cm}^{-1}$. The noticeably different VCD spectrum at pH 3.5, especially in terms of intensity of the signal, is the result of the formation of an aggregated frozen conformation. As mentioned in the Experimental Section, at pH 3.5, the solution becomes extremely viscous, essentially gellike, which may be taken as physical evidence for the formation of the frozen form. Figure 3 also includes the VCD spectrum at pH 3.5 to show the discernible difference between the spectra

of the frozen form versus other acidic forms. The VCD spectral features associated with pH 3.5 reflect the ability of the VCD technique to differentiate the frozen from other acidic forms, which cannot be achieved with ordinary IR absorption spectra. We are not aware of any ECD studies on polyA at pH 3.5. A large increase in VCD intensity with aggregation has been observed³⁷ for DNA, where the aggregation was due to the formation of large dense particles in the presence of Cr³⁺ ions. An increase in ECD intensity was also reported³⁸ for DNA in the presence of poly(ethylene glycol), where aggregation led to compactization of DNA structure.

Since the major VCD features associated with pH values 8.0 and 6.0 appear essentially the same, the transition from single-helical structure to double-helical structure is more evident from the changes in absorption spectra associated with the appearance of band I. On the other hand, VCD features are more indicative of the pH-dependent transitions among the three acidic forms. The appearance of negative VCD contribution at $\sim 1668\text{ cm}^{-1}$ at pH 5.5 and 5.0 indicates the formation of the half-protonated B form. The emergence of the well-defined positive couplet at $\sim 1665\text{ cm}^{-1}$ as well as the disappearance of the positive couplet at $\sim 1628\text{ cm}^{-1}$ reflect the stabilization of a fully protonated A form, at pH 4.5 and 4.0. The high-intensity VCD couplet centered at $\sim 1665\text{ cm}^{-1}$, along with the positive band at $\sim 1614\text{ cm}^{-1}$, is indicative of the frozen form of polyA at pH 3.5. To find out if the temperature-dependent conformational changes are reversible, solution-based spectra were taken at an elevated temperature of $\sim 70\text{ }^{\circ}\text{C}$ for each of the pH values considered and also upon cooling the sample back to room temperature. The aggregated sample, at pH 3.5, was additionally heated to $\sim 110\text{ }^{\circ}\text{C}$, and its spectra were also measured upon cooling the sample back to room temperature.

To facilitate the comparison of the temperature-dependent spectral differences in the pH range 8.0–3.5, the absorption and VCD spectra at elevated temperature (dotted lines) are collected in Figure 3 along with those at room temperature (solid lines). The temperature-induced change when going from 22 to $70\text{ }^{\circ}\text{C}$ that is common to all absorption traces is associated with frequency region IV and is manifested through an increase in the relative intensity as well as through a slight modification in the overall band-shape appearance. As mentioned earlier, the broad unresolved features in region IV may arise from D₂O or HDO, so these changes are probably associated with increased H—D exchange at higher temperature. In the pH range of 6.0–3.5, both bands I and III undergo a decrease in intensity with increasing temperature. Since band I was identified with the double-helix structure, the decrease in intensity of this band with increasing temperature indicates heat-induced partial unfolding of a double helix. Band II undergoes a twofold change as the result of increase in temperature: an increase in its relative intensity at essentially all pH values studied and a shift in its band position to a slightly lower frequency region in the pH range of 8.0–5.0. The VCD couplet associated with absorption band II is also shifted to a slightly lower frequency, but its magnitude is diminished, unlike the associated absorption intensity, in the pH range of 8.0–5.0. At pH 4.5 and below, the shift of band II to a lower frequency region does not occur, and the attenuation of VCD intensity is not as pronounced. The VCD intensity changes for band II suggest that some unfolding of the single helix also takes place as the temperature is increased to $70\text{ }^{\circ}\text{C}$.

The temperature-dependent spectral features seen at $70\text{ }^{\circ}\text{C}$ are reversible because, upon cooling the samples to room temperature, the peaks observed originally at room temperature

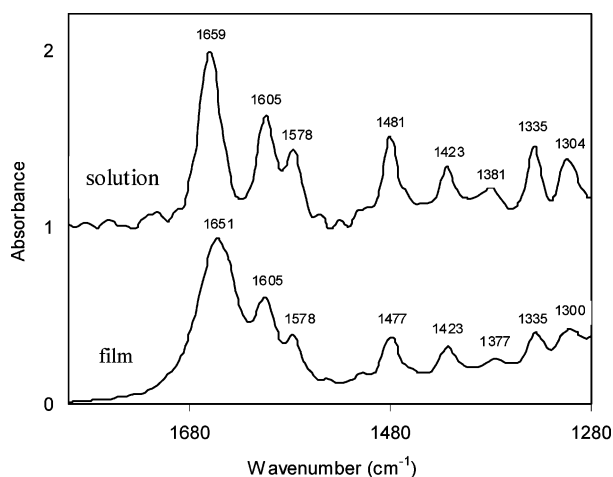


Figure 4. Changes in the absorption features of polyA in going from H₂O solution to a film state. The H₂O solution spectrum was obtained at the same concentration as in Figure 3 for D₂O but using a 6- μ m-path-length cell. The H₂O solvent spectrum was subtracted from the H₂O solution spectrum. The spectra were normalized to unit absorbance.

are restored. It was reported^{3,15} that the melting temperature (T_m) of a solution of polyA at pH 4.25 is about 90 °C. On the basis of this observation, the frozen form at pH 3.5 was also studied at 70 and 110 °C. Although heating of the frozen form to ~70 °C also leads to reversible changes, this compact form is irreversibly disrupted at ~110 °C. The observable transition from a viscous, essentially gellike sample at pH 3.5 and room temperature to a much more fluidlike sample at 110 °C represents clear physical evidence of a conformational transformation at ~110 °C. Cooling back to room temperature does not revert the sample back to gellike appearance, so the disruption of the aggregate form at ~110 °C is an irreversible process. The spectra obtained after heating the aggregated polyA to 110 °C, followed by cooling to room temperature, are also displayed in Figure 3 (topmost traces). A comparison of these spectra with those at initial room temperature at all pH values indicates that these spectra closely resemble those at pH ~4.5, suggesting that the frozen form upon heating to 110 °C converts to the A form. Heating the sample to ~110 °C promotes the separation of aggregated strands and their subsequent recombination into the A form. A smaller influence may also arise from the temperature dependence³⁹ of pH, because upon heating the buffer for 5 min at ~110 °C, the pH of the buffer solution increased from 3.5 to 3.6.

Film State Measurements. Rich et al. have performed the X-ray diffraction study on solid state polyA fibers at a variety of relative humidities to “determine the influence of water on the structure”.³ They found that the diffraction pattern remains essentially completely intact between 100% and 0% relative humidity, suggesting that water has no influence on the fiber structure. To monitor the influence of drying, the absorption spectrum obtained for H₂O solution prepared without buffer is compared to that of the film derived from the same solution in Figure 4. Major changes are not seen as a consequence of drying. The only significant change seen is for the high-frequency band, which shifted from 1659 cm⁻¹ in solution to 1651 cm⁻¹ in the film.

The absorption spectral features observed for the H₂O solution (Figure 4, top trace) are directly comparable to those observed for the film (Figure 4, bottom trace) derived from the same solution. Since VCD spectra cannot be measured for H₂O solution, because of interference from H₂O solvent absorption, one can then undertake VCD measurements for films derived

from H₂O solution. However, such film spectra have not been reported to date for polyA. For this reason we investigated the absorption and VCD spectra for films prepared from buffered parent solutions at the same selection of pH values as explored in the D₂O solution-state study.

The VCD spectra in the film state were reported⁴⁰ previously for proteins and carbohydrates where spectra were found to be independent of rotational orientation of the film around the light beam, but polyA films did not exhibit such rotational independence for VCD spectra, as shown for a representative example at pH 5.5 in Figure 5C' (vide infra). Although the rotational dependence is not always as pronounced as in Figure 5C', the conditions affecting the degree of the rotational dependence are unpredictable, which makes the measurement of VCD spectra of these films unreliable. As discussed in the literature,⁴¹ the rotational dependence for circular dichroism in films originates from linear birefringence and linear dichroism caused by macroscopic orientation or microcrystalline sample formation. In certain cases these unwanted effects and rotational dependence for VCD can be avoided by using matrix-assisted film formation.^{40a} The studies in our laboratory have indicated⁴⁰ that carbohydrates are capable of forming transparent films that can yield rotationally independent VCD spectra. In addition, some literature reports^{42–44} indicated that carbohydrates can act as stabilizing carriers for nucleic acids. Carbohydrates such as lactose, sucrose, dextran, etc. are widely used in the pharmaceutical industry for storage and protection of biochemicals, especially during drying. There are suggestions⁴⁵ that stabilization of solute molecules most likely comes from hydrogen bonding with the matrix.

When polyA is in an aqueous environment, the hydrogen bonding potential associated with hydroxyl groups as well as with nitrogen atoms of polyA is fulfilled via their interaction with hydroxyl groups of water. However, upon evaporation of water during the film formation, such intermolecular hydrogen bonding can be influenced. It is possible that introduction of a carbohydrate matrix, which is rich with hydroxyl groups, can stabilize the polyA sample via intermolecular hydrogen bonding and by minimizing the electrostatic repulsions among phosphate groups. Trehalose is considered⁴⁶ to either replace water molecules for hydrogen bonds or entrap water molecules for bioprotection. For this reason, trehalose-assisted films were prepared for polyA. The optimal ratio for obtaining rotationally independent VCD spectra was determined to be 1:2 (polyA/trehalose). The rotational independence for VCD in polyA films was achieved with a trehalose matrix, as shown in Figures 5A–G, where the frequency region between 1800 and 1500 cm⁻¹ is shown. The region below 1500 cm⁻¹ is not displayed due to interference from trehalose absorption and VCD signals. The main criteria used for assessing the trehalose-containing films is to ensure that the differences between the VCD signals obtained at 0° and 45° positions are within the noise level of the individual VCD spectra. The microscopic images (not shown) of these films indicated uniform and smooth films at higher pH values and somewhat grainy films at lower pH values. Even though the surfaces of the trehalose-containing polyA films become increasingly coarser as the pH is lowered, the quality of the rotational independence for VCD is not compromised at lower pH.

We believe that trehalose acts only as a stabilizing carrier and does not have chemical interaction with polyA for two reasons. First, as seen by the comparison of Figures 5C and 5C' (both at pH 5.5), the addition of trehalose has very little effect on the observed absorbance of polyA. Second, the

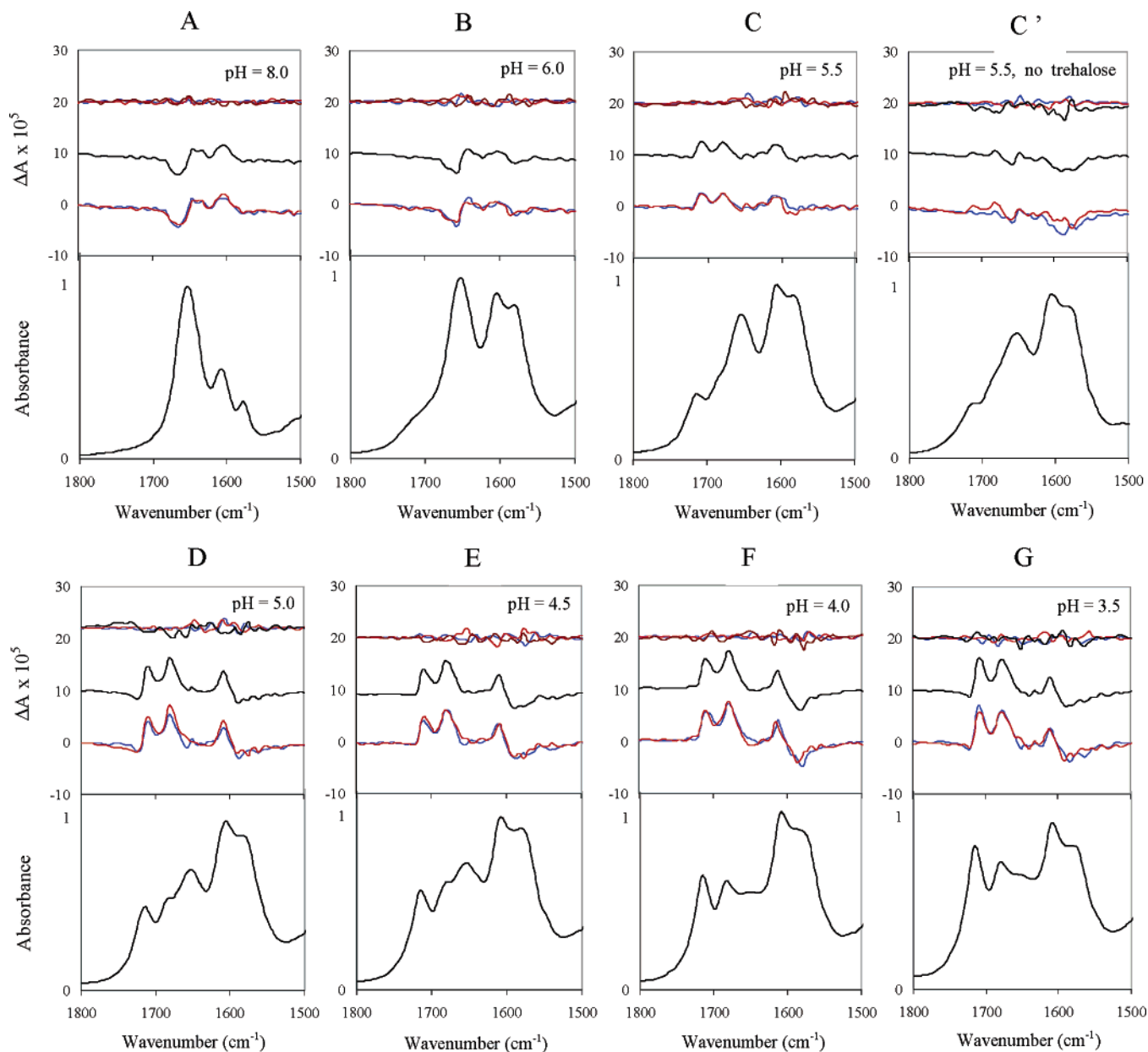


Figure 5. Film-based vibrational absorption (bottom panel) and circular dichroism (top panel) spectra of polyA in the pH range of 8.0–3.5. The top panel displays three sets of traces. The bottom set in the top panel represents traces for VCD spectra obtained at an arbitrarily chosen 0° position (red trace) and at a position obtained via 45° rotation (blue trace) of the film around the light beam axis. The spectra displayed in the middle of the top panel (black trace) represent an average of 0° and 45° VCD spectra. The spectra displayed at the top of the top panel represent traces associated with 0° noise spectra (red trace), 45° noise spectra (blue trace), and the difference between the 0° and 45° VCD spectra (black trace). All spectra, except C', were obtained from parent solutions containing trehalose. The spectrum C' was obtained at pH 5.5 without trehalose. See text for further details.

solution-based absorption and VCD spectra obtained for polyA sample with added trehalose (not shown) are found to be identical to the spectra exhibited by polyA sample without adding trehalose.

Figure 6 displays the progression of absorption (A) and VCD (B) spectral features for film-based samples of polyA, as a function of pH. Absorption bands (as appearing at pH 5.5), ~ 1713 , ~ 1682 , ~ 1655 , ~ 1605 , and ~ 1581 cm^{-1} are labeled as V–IX, respectively. As the pH is lowered, bands V and VI increase, and band VII decreases in intensity. Absorption intensity changes for bands VIII and IX, when going from pH 8.0 to 6.0, are associated with the change of buffer at these two pH values. (The citrate buffer used for the pH range of 6.0–3.5 has absorption features in the region of bands VIII and IX

causing these changes.) There is a slight frequency shift of band VIII from 1605 to 1608 cm^{-1} , when going from pH 5.5 to 5.0.

In the context of correlation between pH-induced changes for the spectral features of solution and film samples, the most notable resemblance is seen (Figure 7) between absorption bands I and II of solution and absorption bands V and VII of films, respectively.

Absorption band I appears in solution at pH 6.0 and becomes gradually intensified as the pH is lowered; similarly absorption band V in film becomes noticeable at pH 6.0 and becomes gradually intensified as the pH is lowered. The position of band I in solution shifts to a higher frequency at lower pH, as does band V of the film. Similarly the position of band II in solution shifts to a lower frequency at lower pH, as does band VII of

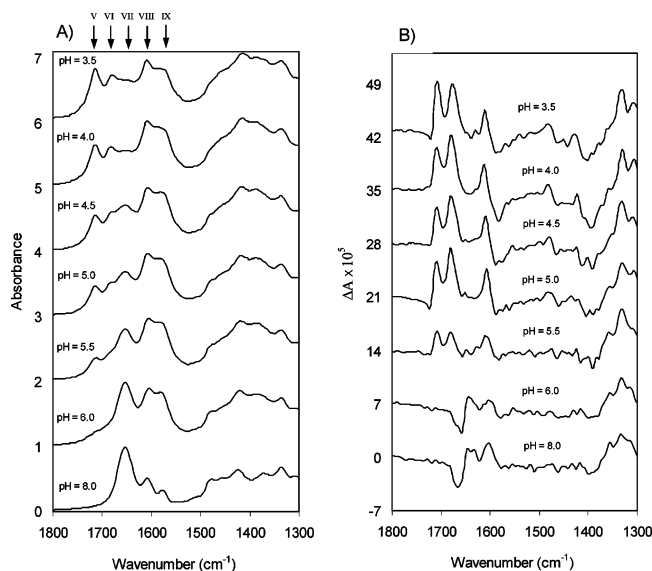


Figure 6. Vibrational absorption (A) and circular dichroism (B) spectra of film samples of polyA, obtained from trehalose-containing parent solutions at pH values of 8.0, 6.0, 5.5, 5.0, 4.5, 4.0, and 3.5. Concentrations used for parent-solution preparations are given in the Experimental Section.

the film. Furthermore, just as the intensity of band II in solution is diminished as the pH of the solution is lowered, the intensity of band VII in film also diminishes as the pH of the parent solution for the film is lowered. The plots (Figure 7) showing dependence of band positions and relative absorption band intensities on pH support these comments. For obtaining relative intensities, band III of the solution and band VI of the film were chosen as the references as their frequencies did not change with pH. The changes in relative band intensities of bands I and II of solution correlate well (Figure 7) with those of bands

V and VII, respectively, of the film. Since occurrence of band I has been identified as the marker of the double-helix formation in solution-based spectra, band V can be considered to indicate the formation of double helix in the film-based spectra.

The VCD features observed for films (Figure 6) at pH values of 8.0 and 6.0 appear to reflect a single-helix structure. As in the solution-state spectra (Figure 3) the film absorption spectrum hints the beginning of the formation of double helix at pH 6.0, in terms of developing a weak band V, and this development has not yet been reflected in the VCD spectrum of the film at pH 6.0. The VCD features for films in the pH range 5.5–3.5 reflect a double-helix structure. Then the single-helix structure is represented by a positive couplet originating from absorption band VII and by a positive band associated with absorption band VIII of the film. The development of the double helix is marked in the film by an abrupt occurrence of the two positive VCD signals, associated with absorption bands V and VI, at pH 5.5 and loss of the positive couplet associated with band VII. As the pH is lowered further and the double helix is reinforced, the positive VCD signals from absorption bands V and VI become more intense, and a negative VCD couplet is formed in region VIII. However, unlike in the solution-state VCD spectra (Figure 3), the distinction between the three acidic forms of polyA, namely, B, A, and frozen forms, is less clear in the film VCD spectra. At pH 3.5 enhanced VCD signals are not seen for films, unlike in solution-state VCD spectra, probably because the concentration of parent solutions used to make films is ~ 3 times smaller than that used for solution-state VCD measurements. As a result, the extent of aggregation in the parent solutions of film samples is less than that in the solutions used for solution-state VCD measurements. For all of the pH values considered, VCD signal magnitudes exhibited by the film samples are considerably weaker than those exhibited by the solution samples.

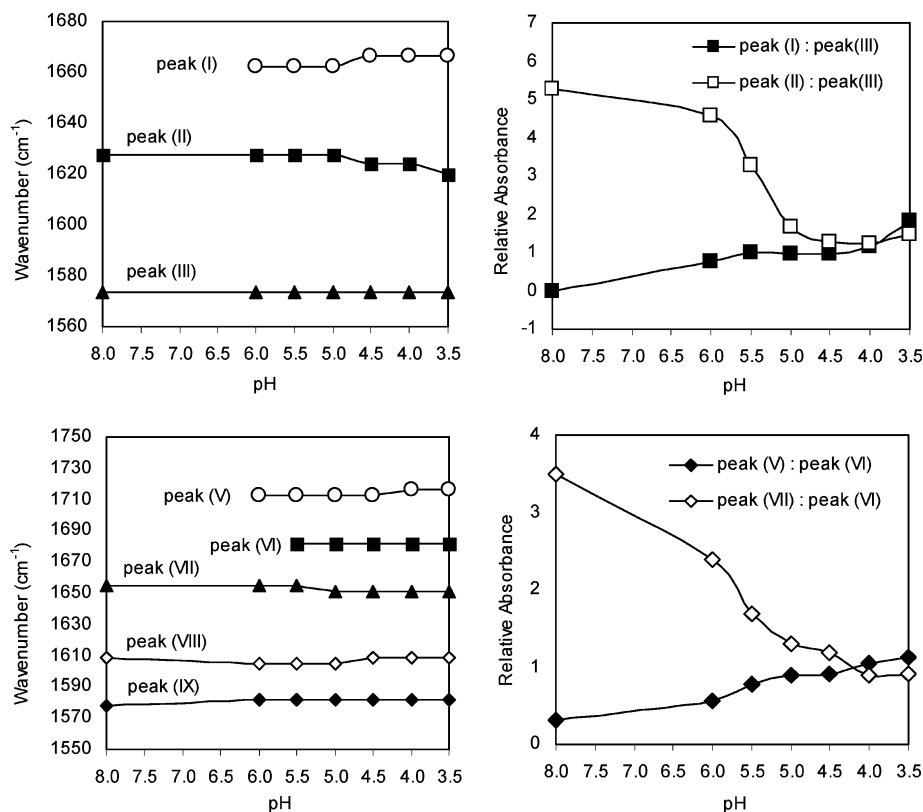


Figure 7. pH-dependent changes in band positions (left two panels) and relative absorption intensities (right two panels) in the solution (top two panels) and film (bottom two panels) spectra.

To confirm the generality of VCD observations for film samples, it is necessary to undertake film studies on different homopolynucleotides that in the solution-state behave similarly to polyA. Since several solution-state homopolynucleotides exhibit VCD band-shape generality, it would be of interest to investigate if similar generality is also reproduced for corresponding films. If the generality turns out to be present, then film-based studies can be used advantageously for nucleic acids.

Conclusions

The present work reports the IR absorption and VCD spectral changes and their correlation to structural changes of polyA as a function of pH in both solution and film states. The analysis of the solution data as a function of pH sheds new light on the previously unrecognized absorption band I at $\sim 1665\text{ cm}^{-1}$ and identifies this band as the marker of the double-helix structure of polyA. The solution spectra additionally demonstrate that the transition from a single- to a double-helical structure is more easily identified from changes in absorption spectra, while the changes in VCD features reflect more transparently the pH-dependent transitions among the three acidic forms of polyA (A form, B form, and frozen form). The solution study also included a temperature-dependent investigation that leads to the conclusion that heating the solution to $\sim 70^\circ\text{C}$ leads to a partial yet reversible unfolding of a single-helix at neutral pH and of a double helix at acidic pH. However, heating of the most acidic frozen form to $\sim 110^\circ\text{C}$ leads to irreversible disruption of the aggregated structure, promoting the separation of aggregated strands and their subsequent recombination into the A form.

We additionally report that rotationally independent VCD spectra can be collected for films of polyA when a trehalose-assisted film formation technique is applied. Trehalose serves as a stabilizing carrier for polyA probably through hydrogen bonding interactions or by trapping H_2O from evaporation. Nevertheless, we believe that changes in IR absorption and VCD spectral features of the film state polyA between pH values of 6.0 and 5.5 are indicative of the transition of the secondary structure from a single to a double helix. It is to be recognized that the spectra of polyA in the film state represent the first step toward realizing the prospect of using film-based spectra in monitoring secondary structural changes for nucleic acids. Believing that the pH-dependent film-based spectra do reflect changes in the secondary structure as observed in solution state, we foresee three instances where films could be used advantageously: (1) in cases where it is difficult to acquire solution spectra because of the limited solubility of polynucleotides, (2) in cases where the solution spectra cannot be collected due to the tendency of certain polynucleotides to form viscous gellike solutions, (3) in cases where the monitoring of polynucleotide structural changes within a natural biological environment (H_2O rather than D_2O) is desired. The present results provide a beginning for the use of the film-based spectra for monitoring the secondary structural changes of polynucleotides. VCD studies on additional polynucleotides, in both solution and film states, are currently being planned to establish the advantage of the film-based spectra as an alternative to the solution-based spectra of nucleic acids.

References and Notes

- (1) Saenger, W. *Principles of Nucleic Acid Structure*; Cantor, C. R., Ed.; Springer-Verlag: New York, 1984.
- (2) Rottman, F. M. *Biochemistry of Nucleic Acids II*; Clark, B. F. C., Ed.; International Review of Biochemistry 17; University Park Press: Baltimore, MD, 1978.
- (3) Rich, A.; Davies, D. R.; Crick, F. H. C.; Watson, J. D. *J. Mol. Biol.* **1961**, *3*, 71–86.

- (4) Luzzati, V.; Mathis, A.; Masson, F.; Witz, J. *J. Mol. Biol.* **1964**, *10*, 28–41.
- (5) Fresco, J. R.; Klemperer, E. *Ann. N. Y. Acad. Sci.* **1959**, *81*, 730.
- (6) Leng, M.; Felsenfeld, G. *J. Mol. Biol.* **1966**, *15*, 455–466.
- (7) Applequist, J.; Damle, V. *J. Am. Chem. Soc.* **1966**, *88* (17), 3895–3900.
- (8) Casassas, E.; Tauler, R.; Marques, I. *Macromolecules* **1994**, *27*, 1729–1737.
- (9) (a) Holcomb, D. N.; Tinoco, I., Jr. *Biopolymers* **1965**, *3*, 121–133. (b) Holcomb, D. N.; Timasheff, S. N. *Biopolymers* **1968**, *6*, 513–529.
- (10) Warshaw, M. M.; Bush, C. A.; Tinoco, I., Jr. *Biochem. Biophys. Res. Commun.* **1965**, *18*, 633–638.
- (11) Sarkar, P. K.; Yang, J. T. *J. Biol. Chem.* **1965**, *240* (5), 2088–2093.
- (12) Poland, D.; Vournakis, J. N.; Scheraga, H. A. *Biopolymers* **1966**, *4*, 223–235.
- (13) Michelson, A. M.; Ulbricht, T. L. V.; Emerson, T. R.; Swan, R. J. *Nature* **1966**, *209*, 873–874.
- (14) Van Holde, K. E.; Brahms, J.; Michelson, A. M. *J. Mol. Biol.* **1965**, *12*, 726–739.
- (15) Brahms, J.; Michelson, A. M.; Van Holde, K. E. *J. Mol. Biol.* **1966**, *15*, 467–488.
- (16) Hashizume, H.; Imahori, I. *J. Biochem.* **1967**, *61*, 738–749.
- (17) Hruska, F. E.; Danyluk, S. S. *J. Am. Chem. Soc.* **1968**, *90*, 3266–3267.
- (18) Chan, S. I.; Nelson, J. H. *J. Am. Chem. Soc.* **1969**, *91*, 168–183.
- (19) Lerner, D. B.; Kearns, D. R. *Biopolymers* **1981**, *20*, 803–816.
- (20) Fresco, J. R.; Doty, P. *J. Am. Chem. Soc.* **1957**, *79*, 3928–3929.
- (21) Stevens, L. C.; Rosenfeld, A. *Biochemistry* **1966**, *5*, 2714–2721.
- (22) McDonald, C. C.; Phillips, W. D. *Science* **1964**, *144*, 1234–1237.
- (23) (a) Brahms, J. *Nature* **1964**, *202*, 797–798. (b) Brahms, J.; Mommaerts, W. F. H. M. *J. Mol. Biol.* **1964**, *10*, 73–88.
- (24) Adler, A. J.; Grossman, L.; Fasman, G. D. *Biochemistry* **1969**, *8* (9), 3846–3859.
- (25) Janik, B.; Sommer, R. G.; Bobst, A. M. *Biochim. Biophys. Acta* **1972**, *281*, 152–168.
- (26) Maggini, R.; Secco, F.; Venturini, M. *J. Chem. Soc., Faraday Trans.* **1994**, *90* (16), 2359–2363.
- (27) Zarudnaya, M. I. *Mol. Biol.* **1998**, *32* (3), 417–422.
- (28) (a) Yang, L.; Keiderling, T. A. *Biopolymers* **1993**, *33*, 315–327. (b) Annamalai, A.; Keiderling, T. A. *J. Am. Chem. Soc.* **1987**, *109*, 3125–3132.
- (29) *Physicochemical Properties of Nucleic Acids*; Dúchense, J., Ed.; Academic Press: New York, 1973; Vol. 2.
- (30) Xiang, T.; Goss, D. J.; Diem, M. *Biophys. J.* **1993**, *65*, 1255–1261.
- (31) Polavarapu, P. L.; Zhao, C. *Fresenius J. Anal. Chem.* **2000**, *366*, 727–734.
- (32) Andrushchenko, V.; Wieser, H.; Bour, P. *J. Phys. Chem. B* **2004**, *108*, 3899–3911.
- (33) (a) Wang, L.; Pancoska, P.; Keiderling, T. A. *Biochemistry* **1994**, *33* (28), 8428–8435. (b) Wang, L.; Yang, L.; Keiderling, T. A. *Biophys. J.* **1994**, *67*, 2460–2467. (c) Wang, L.; Keiderling, T. A. *Nucleic Acids Res.* **1993**, *21* (17), 4127–4132.
- (34) Self, B. D.; Moore, D. S. *Biophys. J.* **1997**, *73*, 339–347.
- (35) Diem, M. *Introduction to Modern Vibrational Spectroscopy*; John Wiley and Sons: New York, 1993.
- (36) Gunzler, H.; Gremlich, H. U. *IR Spectroscopy*; Blumich, M. J., Translator; Wiley-VCH: Weinheim, Germany, 2002.
- (37) Andrushchenko, V.; Leonenko, Z.; van de Sande, H.; Wieser, W. *Biopolymers* **2002**, *61*, 243–260.
- (38) Evdokimo, Yu. M.; Platonov, A. L.; Tikhonenko, A. S.; Varshavsky, Ya. M. *FEBS Lett.* **1972**, *23*, 180–184.
- (39) Westcott, C. C. *pH Measurements*; Academic Press: New York, 1978; p 102.
- (40) (a) Shanmugam, G.; Polavarapu, P. L. *Appl. Spectrosc.* **2005**, *59*, 673–681. (b) Shanmugam, G.; Polavarapu, P. L. *J. Am. Chem. Soc.* **2004**, *126*, 10292–10295. (c) Petrovic, A. G.; Bose, P. K.; Polavarapu, P. L. *Carbohydr. Res.* **2004**, *339*, 2713–2720.
- (41) Harada, T.; Kuroda, R. *Chem. Lett.* **2002**, 326–327.
- (42) Mueller, O.; Deuter, R. German Patent Application DE 95-19530132 19950816, 1997.
- (43) Maruyama, A.; Akaike, T.; Goto, T.; Yonemura, K. Japanese Patent 96-146825 19960516, 1998.
- (44) Debenedetti, P. G.; Errington, J. R.; Feeney, M. R. Preservation of biomolecules in carbohydrate–water glasses. In *Abstract of Papers*, 221st ACS National Meeting, San Diego, CA, April 1–5, 2001; American Chemical Society: Washington, DC, 2001.
- (45) Lopez de la Paz, M.; Gonzalez, C.; Vicent, C. *Chem. Commun.* **2000**, 411–412.
- (46) Mei, E.; Tang, J.; Vanderkooi, J. M.; Hochstrasser, R. M. *J. Am. Chem. Soc.* **2003**, *125*, 2730–2735.